Hydrodynamics of wind-assisted ship propulsion verification and validation of RANS methodology

van der Kolk, Nico; Keuning, Lex; Huijsmans, Rene

Publication date
2016

Document Version
Final published version

Published in
Proceedings of the12th International Conference on Hydrodynamics-ICHD 2016

HYDRODYNAMICS OF WIND-ASSISTED SHIP PROPULSION
VERIFICATION OF RANS SIMULATIONS

N.J. van der Kolk, J.A. Keuning and R.H.M. Huijsmans
Ship Hydromechanics, TU Delft
Mekelweg 2, 2628 CD Delft, The Netherlands
N.J.vanderKolk@tudelft.nl, J.A.Keuning@tudelft.nl, R.H.M.Huijsmans@tudelft.nl

ABSTRACT: Wind-assisted ship propulsion is under study at the Delft University of Technology. This alternative propulsion is gaining attention due to increased concern for the environment. For designers who are considering the potential benefits of this new option, a well-founded performance prediction tool is a key prerequisite. Together with Politecnico Milan, the TU Delft is developing such a tool, which will allow for inexpensive assessment of wind-assist concepts using regression based force models. Reynolds-Averaged Navier Stokes (RANS) simulations will be a primary tool during this study. The advent of the numerical towing tank brings possibilities but also new challenges. The predominance of large, separated flow structures in the wake of the sailing ship, and the particular interest in the lateral force generation of the hull, points to a conscientious grid verification study. Here, it is sufficient to achieve parity among uncertainty contributions within the larger context of the project. Diverse procedures are available for evaluating the numerical uncertainty of a RANS simulation. Principal methods were defined and implemented for verification cases at leeway angles of 0, 9, and 20 degrees. The uncertainty for lateral force at 9 degrees leeway for the base grid (2E6 cells) was estimated to be 8.3%.

INTRODUCTION

Wind energy as an auxiliary form of propulsion for commercial ships has again become of great interest as a possible response to volatile fuel prices and increasingly stringent environmental regulations. A well-founded performance prediction tool is a key prerequisite for the further development of this promising technology, and with the support of the European Commission and others, a group of researchers at Delft University of Technology is developing a performance prediction program for these hybrid ships. The Wind-Assisted Ship Propulsion (WASP) performance prediction tool will provide designers the ability to explore the possibilities offered by wind as an auxiliary propulsor. The aim is to deliver a regression-based force model that is applicable to a broad range of vessels. The WASP performance prediction program will allow for parametric investigations, and eventually for the optimization of commercial hull forms for sailing. The expansion and refinement of the force models is the subject of ongoing work at Delft University of Technology.

Fitting a commercial vessel with an auxiliary wind propulsor will introduce a set of forces and moments besides the desired aerodynamics thrust. The ship will sail with a leeway angle β about the yaw axis, equivalent to the angle of attack for the hull, in order to generate the hydrodynamic reaction in opposition to the transverse component of the aerodynamic force. Further, the distribution of the hydrodynamic sideforce along the hull may result in a net yaw moment. At last, the vertical separation between the sideforce components will create a heeling moment. As hybrid vessels, the performance of a wind-assist concept will depend on the contribution of the wind propulsor, alongside the efficiency of the conventional propulsion system and the drag penalty associated with heel and leeway: the “sailing

condition". Of course, the introduction of a sail-plan will only benefit the vessel if the net thrust gained outweighs any loss in efficiency or increase in resistance.

In the service of regression analysis, the Reynolds-averaged Navier Stokes (RANS) package FINE/Marine is used to assess hull variants. Simulation verification for integrated quantities on the bare-hull at model scale will be described here. The large, separated flow structures in the wake of the sailing ship, and the particular interest in the transverse force has complicated the verification process; in discerning between (perhaps substantial) modelling errors and numerical errors. Taking the larger view, the sideforce is a central component in the larger evaluation for the performance of a wind-assist vessel. The uncertainty level for the prediction of hydrodynamic lateral force should reflect the large impact of this component on the fidelity of the performance prediction.

RANS CFD VERIFICATION PROCEEDURES

Methodology

Several governing bodies publish standards for simulation verification, including the International Towing Tank Committee (ITTC) [1] and the American Society of Mechanical Engineers (ASME) [2]. The Grid Convergence Index (GCI) of Roach is commonly accepted, thanks in part to his strong advocacy for standardization of journal policies regarding uncertainty reporting for computational fluid dynamics. His influence is seen throughout subsequent work on this topic. The ITTC recommendations include the correction factor method of Stern [3] as well as the GCI.

A numerical simulation will have some error associated with spatial discretization. The behavior of the solution for increasing mesh refinement may be separated into two regions: the stochastic range and the asymptotic range [4]. The resolution to which a given problem is solved will determine the extents of the stochastic range, in which some degree of scatter is present in solutions for varying grid refinement. When flow features are sufficiently resolved, the simulation will converge asymptotically with further grid refinement. Most CFD verification methodologies are predicated on the convergence behavior in this asymptotic range. This concept has origins in the work of Richardson [5], who identified the asymptotic approach to a continuum solution for finite difference calculations with increasing grid refinement.

Several practical issues complicate the application of uncertainty estimation procedures, chief among which is the definition of a family of systematically refined grids that lies within the asymptotic range and yet remains computationally feasible. Among the procedures, diverse approaches are taken to overcome this limitation. In an attempt to reach a consensus for the uncertainty estimation for CFD simulations, the following methodology is adopted [6]:

1 Uncertainty estimates are calculated (when possible) according to the methods described below, for multiple sets of grids.

2 The estimates are averaged to arrive at a 'consensus' value for the uncertainty.

Grid Convergence Index

The so-called Richardson extrapolation was adopted by Roach [7] to estimate the uncertainty due to spatial and temporal errors in CFD. Beginning with the generalized Richardson extrapolation:

$$f_0 \cong f_1 + \frac{f_1 - f_2}{r^p - 1} \tag{1}$$

$r = \frac{h_2}{h_1}$ is the grid refinement ratio for a characteristic grid height h. This is an expression for the function value at zero-grid spacing, based on the function value at a series of geometrically similar grids. The exponent p is either the theoretical or observed order of convergence. The difference $\delta_{RE} = f_0 - f_1$ is an estimate of the error for grid one, corresponding to a 50% uncertainty band when this value is interpreted as a single realization of that error. Thus:

$$U_{50\%} = \delta_{RE} = \frac{f_1 - f_2}{r^p - 1} \tag{2}$$

One might argue that δ_{RE} is derived from multiple realizations of the function: $f_1,\ f_2$. Finally, to extend the confidence interval to 95% Roach defines the Grid Convergence Index (GCI) as:

$$GCI = F_s * |\delta_{RE}| \tag{3}$$

F_s is interpreted as the coverage factor or, in engineering parlance, as the factor of safety. Roach suggests $F_s = 3$ for rudimentary grid convergence studies involving two grids, and $F_s = 1.25$ for more rigorous studies.

The efforts of Roach have been carried further by Eça [8] [9], who has applied a least-squared approach to accommodate data scatter within the stochastic range. Eça also incorporates the error estimates of Oberkampf [10], when data scatter is such that reliable estimates for the order of convergence, p, are not feasible. In these cases, convergence is assumed to proceed with either first or second order, or with mixed order.

$$\delta_1 = ch \tag{4}$$

$$\delta_2 = ch^2 \tag{5}$$

$$\delta_{12} = c_1 h + c_2 h^2 \tag{6}$$

Also, recognizing that practical ship flows CFD applications preclude the true approach to the asymptotic range while using three systematically refined grids, Eça proposes a weighting within the least squared minimization that favors the fine-grid solutions.

A selection is made among the available error estimates based on the observed order of convergence and the standard deviation for each fit. For cases where p is much greater or less than the expected order of convergence, the power-series estimate according to Oberkampf that best fits the data is selected, with an increased $F_s = 3$. Once the error estimate has been selected, it is used to determine the uncertainty by considering the data scatter, Δ_ϕ, the degree to which the data behavior conforms to the error estimator (standard deviation of the fit), and

the difference between the data value and the fit. A full description of this procedure is given in Eça [8].

$$\mathbf{U_{GCI}} = \begin{cases} \boldsymbol{F_s\delta_i + \sigma + \left|\phi_i - \phi_{fit}\right|} & \boldsymbol{\sigma < \Delta_{phi}} \\ \boldsymbol{3\sigma/\Delta_\phi\left(F_s\delta_i + \sigma + \left|\phi_i - \phi_{fit}\right|\right)} & \boldsymbol{\sigma \geq \Delta_{phi}} \end{cases} \tag{7}$$

U_{GCI} is labeled as such due to its close relationship to the original GCI proposed by Roach [7].

Correction Factor

In a parallel development, Stern and Wilson [11] have proposed an adaption to the Richardson extrapolation that assigns weights according to the observed order of convergence. This correction factor method is presented alongside the GCI of Roach in the ITTC recommended practices for CFD simulation verification [1]. The correction factor may be interpreted as an elaborated safety factor. The correction factor compares the observed rate of convergence with the theoretical order for the simulation and as a measure of the proximity of the grids used to the asymptotic range.

$$C = \frac{r^p - 1}{r^{p_{est}} - 1} \tag{8}$$

Where r and p are determined from a set of grids using the least-squares technique. If the observed order, p, is equal to the estimated order then C is unity. For solutions outside the asymptotic range ($C \neq 1$), the sign and magnitude of C is used to determine the uncertainty according to:

$$U_C = \begin{cases} [9.6(1-C)^2 + 1.1]|\delta_{RE}| & |1-C| < 0.125 \\ [2|1-C| + 1]|\delta_{RE}| & |1-C| \geq 0.125 \end{cases} \tag{9}$$

The final form of equation (17) has developed from communications between Stern et al. [3] [11] and Roach, the product of which being that these approaches exhibit comparable behavior. For example, for the limit as $C \to 1$, $U = 1.1|\delta_{RE}|$.

Approximate Error Scaling

In a series of publications, [6] [12] [13], Celik has advanced the Approximate Error Scaling (AES) method for quantifying the uncertainty of CFD simulations. The premise of this approach is that the error at grid level i is proportional to the approximate error, a function for the change in simulation value with successive grid refinement. Similar to the construction of the error within the GCI formulations, the quantity $|\phi_i - \phi_0|$ is estimated using a power series expansion for (αh), wherein the reciprocal of the refinement ratio $\alpha = \frac{1}{r}$ is used. A set of successively refined grids has the characteristic lengths $[h_1, h_2, h_3]$ such that $\alpha^2 h_1 = \alpha h_2 = h_3$. The expansion reads:

$$E_e(\alpha, h) = \phi(\alpha h) - \phi(0) = \sum_{k=1}^{\infty} a_k \alpha^k h^k \tag{11}$$

Defining also the approximate error E_a as the change in simulation value for progressive grid refinement by factor α:

$$E_a(\alpha, h) = \phi(\alpha h) - \phi(h) = \sum_{k=1}^{\infty} a_k(\alpha^k - 1)h^k \tag{12}$$

Finally, the extrapolated error, E_e is written in terms of the approximate error (as opposed to the numerical solution):

$$E_e(\alpha, h) = \frac{1}{1 - \frac{\sum_{k=1}^{\infty} a_k h^k}{\sum_{k=1}^{\infty} a_k \alpha^k h^k}} E_a(\alpha, h) \tag{13}$$

The further evaluation of the right-hand-side is given in [6]. Simulation data for a set of systematically refined grids is used to define a cubic spline for the approximate error $E_a(\alpha, h)$. The associated uncertainty is estimated:

$$U_{AES} = 1.1 * ERE \tag{14}$$

The behavior for the approximate error (including its derivative), as h approaches zero, is additional information used in this method, over the input for methods based on the Richardson Extrapolation above. According to Celik, the exceptional performance of this method is attributed to this additional information about the behavior of the error in the limit for zero-grid size. [13]

GRID GENERATION

Simulation verification as described above requires a set of grids that are geometrically similar and cover a range of grid sizes within the asymptotic range. Defining a set of grids is complicated by the unstructured nature of the FINE/Marine grid, and by the presence of boundary layer cells for typical ship flow simulations. Geometric similitude is achieved in the simplest sense by progressive subdivision of mesh cells. For three-dimensional problems, the resulting grids will exceed computing limits, and a compromise is necessary according to the available computational power. Particular interest in the sideforce generated by a ship with leeway angle, which is a product of massive flow separation and a wake of vortical structures passing around the hull, has led to an emphasis on the refinement diffusion when compromise was needed.

Systematic grid refinement for a family of grids is achieved by varying initial cell subdivision and refinement diffusion. In Hexpress, each surface is assigned a refinement level and refinement diffusion, which specify the number of times that adjacent cells are subdivided and the thickness of each refinement level, respectively. The refinement levels remain constant across all grids, so the initial cell subdivision defines the cell size for each grid. Refinement diffusion should double with each grid subdivision, and this has been adhered to insofar as possible. The time step for simulations was scaled with the cell size to maintain a constant Courant number (C), used by numerical schemes for the flow gradient and for the phase equation at the free surface. Mesh construction details are presented in table 1.

An unstructured mesh for three-dimensional, complex geometries requires a definition for grid size. This dimension must be a length that is descriptive of the grid, and should decrease monotonically for a set of grids, preferably with constant refinement ratio r. Roach suggests the following:

$$h_{vol} = \sqrt[3]{\frac{vol}{N}} \tag{15}$$

In which vol is the volume of the computational domain and N the number of cells. This definition for cell height is global quantity: it does not reflect the distribution of cells throughout the domain according to the refinement diffusion, which is of particular importance for capturing flow structures around the hull. As a consequence of this ambiguity in the cell height metric, the observed order of convergence may not agree with the theoretical order of convergence. In other words, a second-order numerical scheme which is expected to converge with $(dx)^2$ may not behave accordingly with $(h_{vol})^2$.

The viscous layers, which must satisfy physical modeling requirements and cannot be scaled with the grid, will disrupt grid similitude. Some compromises were needed to construct the meshes while satisfying the requirements of the log-law wall model. The initial cell height was chosen to maintain $30<Y^+<100$ in so far as possible. Due to the recirculation region near the transom, Y^+ values smaller than 15 were present for approximately 1.5% of the hull wetted surface. The maximum Y^+ along the leading bilge was considered to be the driving consideration, as separation is expected at that location. Simulations are carried out at model scale, with a relatively low Reynold's number of 2.3E6, and the requirements of the log-law wall model were quickly satisfied with increasing grid refinement (see table 1). Two families of grids are defined as [1,2,3,4] and [1vl,2vl,3vl,4], so that the first set does not contain viscous layers. For grid 3, the compromise between cell height and diffusion refinement is apparent in the cell height, which is larger than desired for Y^+.

Mesh	**Number of Cells N**	**Ref. Diffusion**	h_{vol}	**Initial Cell Height**	**Viscous Cells**	**Mean Y^+ (max)**	**Max C (FS)**
1vl	7.3E+05	2	1.00	4.29E-03	5	60.4 (93)	5.5 (3.4)
1	8.8E+05	2	0.94	4.29E-03	-	51 (114)	4.0 (1.8)
2vl	1.1E+06	3	0.88	4.29E-03	5	52.2 (86)	5.9 (2.8)
2	1.4E+06	3	0.81	4.29E-03	-	53 (117)	3.8 (2.1)
3vl	2.0E+06	5	0.71	4.29E-03	3	42.5 (84)	5.4 (1.8)
3	2.6E+06	5	0.65	4.79E-03	-	53.1 (110)	4.7 (1.9)
4	8.8E+06	10	0.44	3.22E-03	-	40.8 (84)	2.9 (1.5)

Table 1 – Details of Mesh Construction

TURBULENCE MODELING

The task of modeling large-scale turbulent structures removed from the hull, such as separated bilge vortices, may challenge the assumptions made when averaging the Navier-Stokes equations. However, with the premium placed on economical simulations, it is considered impractical to include large-eddy simulation in the routine evaluation of hull variants. Following the same reasoning, time-averaging an unsteady simulation is not considered here. It is understood that flow around the hull will include large anisotropic vortices that will play a key role in the sailing performance of the hull. Turbulence is modeled with the Explicit Algebraic Stress Model (EASM), providing a balance between the Boussinesq-modeling and the modeling of Reynolds stresses and giving a more physical approach while remaining viable within the scope of work and for the computational resources available.

SIMULATION VERIFICATION

The parent hull of the 1st wind-assist systematic series is used for this verification exercise. The lines plan for the bare hull is given in figure 1. The simulation is performed at Fn=0.168, equivalent to 12 knots at full scale, and at 0, 9, and 20 degrees leeway. In total, 21 calculations were performed on 7 grids. Integrated fluid forces on the model are determined in the coordinate system aligned with the direction of forward motion. The uncertainty estimates for 9^o leeway are presented in detail.

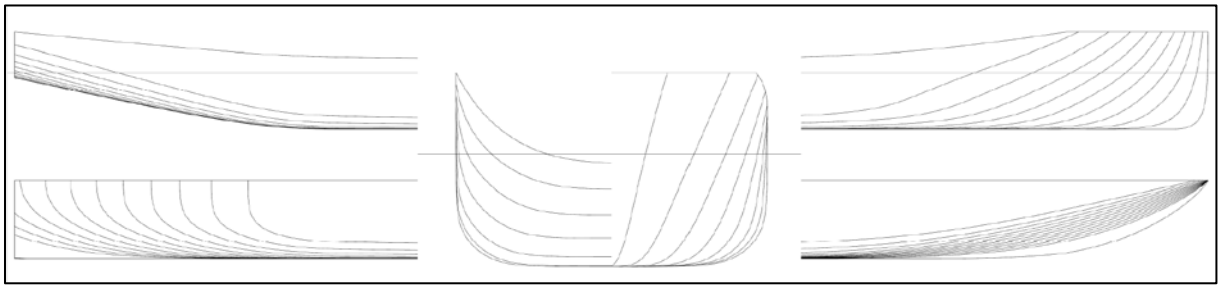

Figure 1 – Lines plan for verification case

The uncertainty for resistance is computed using the viscous-layer grids. The observed order of convergence was 3.8, resulting in exaggerated values for U_C, which have been omitted. Wall distance requirements for the no-VL grids were not strictly adhered to. For this case and for the yaw moment (table 4), the GCI formulation switches to the power series expressions (Oberkampf [10]), implying that the observed order is no longer reliable for error estimates with the correction factor.

Mesh	U_{GCI}	U_C	U_{EAS}	$\bar{U}_{X9}$
1	17.8%	-	16.4%	17.1%
2vl	6.9%	-	6.1%	6.5%
3vl	4.9%	-	4.7%	4.8%
4vl	0.4%	-	2.8%	1.6%

Table 2 – Relative uncertainty estimates for resistance (9^o leeway)

The uncertainty estimation for sideforce is compelling. The broad agreement among the uncertainty formulations and between the two sets of grids suggests that the derived values are reliable. The observed order of convergence for the grid set without viscous layers was 2.3, while for the viscous layer set it was 2.5. The influence of boundary layer meshing on the convergence behaviour and the uncertainty estimate is apparent. The results for yaw moment are also congruent, though some numerical issues arose due to the low observed order of convergence (p =0.6).

Mesh	U_{GCI}	U_C	U_{EAS}	**Mesh**	U_{GCI}	U_C	U_{EAS}	$\bar{U}_{Y9}$
1	7.0%	6.9%	6.8%	**1vl**	19.4%	30.2%	17.3%	14.6%
2	4.8%	5.0%	6.2%	**2vl**	14.3%	22.0%	14.5%	11.2%
3	2.5%	3.0%	5.1%	**3vl**	9.3%	14.0%	15.7%	8.3%
4	0.4%	1.2%	2.5%	**4**	2.9%	4.1%	10.0%	3.5%

Table 3 – Relative uncertainty estimates for sideforce (9^o leeway)

Mesh	U_{GCI}	U_C	U_{EAS}	**Mesh**	U_{GCI}	U_C	U_{EAS}	$\bar{U}_{N9}$
1	11.3%	-	-	**1vl**	11.6%	-	-	11.5%
2	11.8%	-	8.0%	**2vl**	11.6%	-	12.0%	10.9%
3	12.2%	-	7.0%	**3vl**	10.9%	-	10.6%	10.2%
4	10.3%	-	3.7%	**4**	8.4%	-	6.2%	7.1%

Table 4 – Relative uncertainty estimates for yaw moment (9^o leeway)

Finally, the analysis is extended to the case for 20^o leeway, where it is expected that the threshold between the stochastic and asymptotic range may shift as separated flow structures becomes larger and more energetic. In fact, the methods outlined in this paper do not succeed for the sideforce indicating that the modelling errors in the simulation are such that simulation convergence for grid refinement is not possible.

CONCLUSION

The discretization uncertainty for integrated forces on the ship hull has been established for bare hull configurations. The verification exercise described herein is a needed prerequisite for the reliable assessment of hull-form variants using CFD simulations. The verification has been conducted with particular focus on the hydrodynamic sideforce, as a leading component of the hydromechanics of wind-assisted ships. Based on the results, the uncertainty procedure developed by Eça, based on the GCI of Roach, was the most robust approach. The correction method was highly susceptible to the observed order of convergence, and the AES was complicated by some numerical issues associated with finite differencing. Estimates for simulation uncertainty are tabulated below.

Mesh	U_{X0}	U_{X9}	U_{Y9}	U_{N9}	U_{X20}	U_{Y20}	U_{N20}
1	24.0%	17.1%	14.6%	11.5%	17.0%	-	28.8%
2	8.6%	6.5%	11.2%	10.9%	11.3%	-	28.0%
3	2.6%	4.8%	8.3%	10.2%	7.9%	-	27.4%
4	0.5%	1.6%	3.5%	7.1%	2.8%	-	22.3%

Table 5 – Overview of numerical uncertainty estimates

Calculated uncertainty for the transverse force is congruent for all methods and across both sets of grids. Improvement in geometric similarity for grids without viscous layers gave better-behaved convergence, and resulted in lower uncertainty estimates. Both the order of convergence and the standard deviation for the least-squares fit for the no-VL grid set were superior to the viscous layer set (see figure 2). Details for the approximate error scaling method are also given in figure 2. The evaluation of derivatives while computing eq. 13 resulted in some numerical issues, as seen near cell size $h = 1$. Still, there is broad agreement between uncertainty values for the methods implemented. Larger uncertainties obtained with the VL grid set are retained because these grids represent the likely grids used in practical calculations.

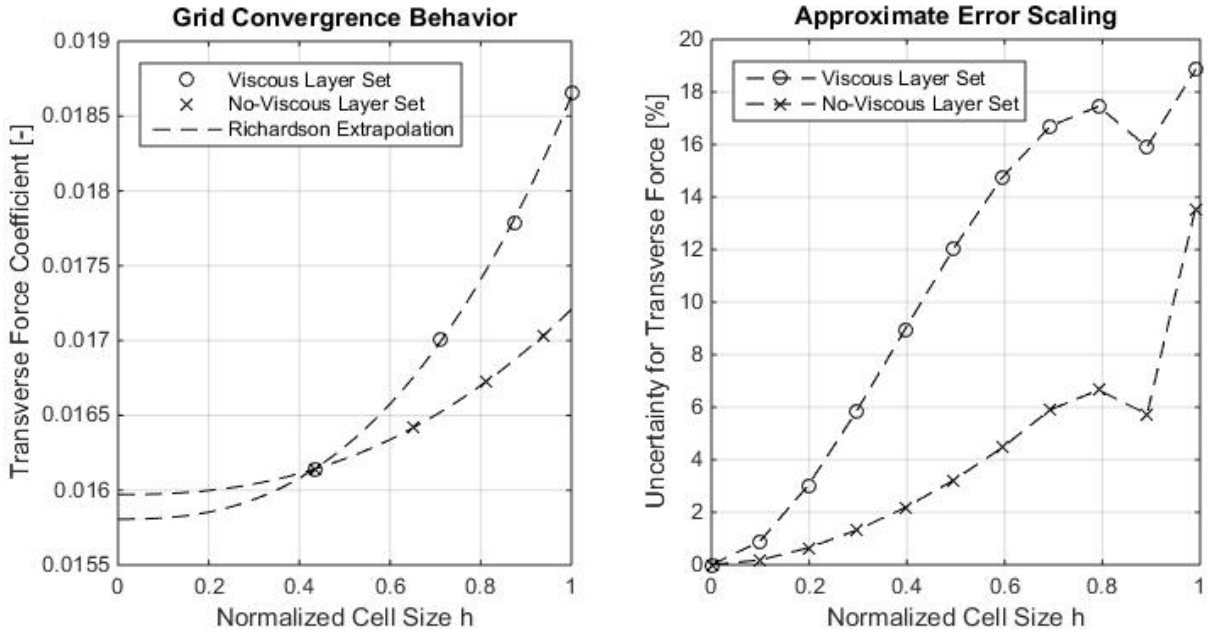

Figure 2 — Convergence behavior and AES uncertainty for transverse force component

Further steps in this work will include the validation for bare hull cases, and the simulation of the appended hull.

REFERENCES

[1] Internation Towing Tank Commitee, "Recommended Practices- Uncertainty Analysis in CFD Verification Proceedures," 2008.

[2] American Society of Mechanical Engineers, "Standard for Verification and Validation in Computational Fluid Dynamics and Heat Transfer," ASME, 2009.

[3] F. Stern, R. Wilson, H. . Coleman and E. Paterson, "Comprehensive Approach to Verification and Validation of CFD Simulations--Part 1: Methodology and Procedures," *Journal of Fluids Engineering,* pp. 793-810, 2001.

[4] I. M. Viola, P. Bot and M. Riotte, "On the Uncertainty of CFD in Sail Aerodynamics," *International Journal for Numerical Methods in Fluids,* vol. 72, pp. 1146-1164, 2013.

[5] L. Richardson, "The Deferred Approach to the Limit," *Transactions of Royal Society London,* vol. 226, pp. 299-361, 1927.

[6] B. Celik and J. Li, "Assessment of Numerical Uncertainty for the Calculations of Turbulent Flow over a Backward-facing Step," *Internaional Journal for Numerical Methods in Fluids,* vol. 49, pp. 1015-1031, 2005.

[7] P. J. Roach, "Quantification of Uncertainty in Computational Fluid Dynamics," *Ann. Rev. of Fluid Mechanics,* vol. 29, pp. 123-160, 1997.

[8] L. Eça and M. Hoekstra, "A Proceedure for the Estimation of the Numerical Uncertainty of CFD Calculations Based on Grid Refinement Studies," *Journal of Computational Physics,* vol. 262, pp. 104-130, 2014.

[9] L. Eça, V. Guilherme and M. Hoekstra, "Code Verification, Solution Verification, and Validation in RANS Solvers," *Proceedings ASME Conference ence on Ocean, Offshore, and Arctic Engineering,* 2010.

[10] W. L. Oberkampf, "A Proposed Framework for Computational Fluid Dynamics Code Calibration/Validation," *AIAA,* no. 94-2540, 1994.

[11] F. Stern, R. . Wilson and J. Shao, "Quantitative V&V of CFD Simulations and Certification of CFD Codes," *International Journal for Numerical Methods in Fluids,* vol. 50, pp. 1335-1355, 2005.

[12] I. Celik and O. Karatekin, "Numerical Experiments on Application of Richardson Extrapolation with Nonuniform Grids," *Journal of Fluids Engineering,* vol. 119, pp. 584-590, 1997.

[13] I. Celik, J. Li, G. Hu and C. Shaffer, "Limitations of Richardson Extrapolation and some Possible Remedies," *Journal of Fluids Engineering,* vol. 127, pp. 795-805, 2005.

[14] H. Coleman and F. Stern, "Uncertainties and CFD Code Validation," *Journal of Fluids Engineering,* pp. 795-803, 1997.